Available online at www.sciencedirect.com
ScienceDirect
International Journal of Thermal Sciences 47 (2008) 1442–1453
International Journal of Thermal Sciences
www.elsevier.com/locate/ijts

Modelling of transport processes and associated thermodynamic irreversibilities in ignition and combustion of a pulverized coal particle

S.S. Mondal *

Department of Mechanical Engineering, Institute of Technology, BHU, Varanasi 221005, India

Received 22 September 2006; received in revised form 7 December 2007; accepted 8 December 2007

Available online 25 January 2008

Abstract

A comprehensive mathematical model of various physical processes and associated thermodynamic irreversibilities of combustion of a pulverized coal particle in the surrounding of a quiescent hot gas has been developed. The model is based on the solutions of spherico-symmetric conservation equations of heat, mass and momentum transport in both the gas and solid phases in consideration of homogeneous and interphase heterogeneous chemical reactions. The reactions are assumed to be irreversible ones and have been considered by suitable models of chemical kinetics. The thermodynamic irreversibilities due to transport processes and chemical reactions in gas phase have been determined from the generalized entropy conservation equation. The influences of coal particle diameter, coal composition and the free stream gas phase temperature on (i) temperature and life histories of burning coal particles, (ii) possible ignition states and (iii) temporal variations of process irreversibilities have been established.
© 2007 Elsevier Masson SAS. All rights reserved.

Keywords: Pulverized coal; Combustion; Ignition; Process irreversibility

1. Introduction

The coal is an important source of energy in generating electricity and also to meet its future demand since the coal reserves are much greater than those of other fossil fuels. Most of the coal fired thermal power plants use pulverized coal for combustion. The coal is also used in the operation of a blast furnace which employs pulverized coal injection along with blast air through its tuyere to reduce the coke feed rate. The pulverization of coal into fine particles are made to increase the specific surface area (the ratio of surface area to volume) to enhance the rate of heat and mass transfer between the coal particles and surrounding hot gas. An efficient and stable combustion of pulverized coal particles depends upon the physical and chemical properties of coal, the diameter of coal particles and other operating conditions like temperature, pressure and fluid-dynamic state of the surrounding gas.

The scope of coal combustion is very wide and well diversified. Host of articles, both numerical and experimental in nature, are available in literature on the studies of pulverized coal combustion.

The important experimental studies [1–8] pertain to the combustion of pulverized coal in different types of combustor at different operating conditions. The studies deal mainly with the influence of coal composition on thermal decomposition of coal and different stages of coal combustion like devolatilization, char combustion etc. Recognition of rate determining process, determination of the reaction rate constants, are mainly the characteristic features of the studies. Some of the works [5,6] also aim at identification of species as emissions and determination of their concentration levels.

On the other hand, a large number of numerical works [9–21] have been made to model the different stages of coal combustion process. States of art documents [22,23] on combustion modeling are also available in literature. It is pointed out in these documents that model development has not yet reached the point where significant use is made in the development process for coal combustion. However attention has been paid to different aspects of combustion modeling like reaction kinet-

* Tel.: +915422368157 (office); +919838542109 (mobile).
E-mail address: mondal_1976@yahoo.com.

1290-0729/$ – see front matter © 2007 Elsevier Masson SAS. All rights reserved.
doi:10.1016/j.ijthermalsci.2007.12.005

Nomenclature

a	radius of the particle at any instant	m	
A	pre-exponential factor	s^{-1}	
c_p	specific heat at constant pressure	$J\,kg^{-1}\,K^{-1}$	
C	mass fraction of species		
d	diameter of the particle	m	
D	diffusivity of species in ambience	$m^2\,s^{-1}$	
E	activation energy	$J\,kg^{-1}$	
G	irradiation	$W\,m^{-2}$	
ΔH_{vap}	enthalpy of vaporization of water	$J\,kg^{-1}$	
ΔH_{vol}	enthalpy of devolatilization during pyrolysis	$J\,kg^{-1}$	
ΔH_{char}	enthalpy of char reaction	$J\,kg^{-1}$	
K	thermal conductivity	$W\,m^{-1}\,K^{-1}$	
m	mass	kg	
M	molecular weight	$kg\,kg\,mol^{-1}$	
P	pressure	Pa	
P_v	vapour pressure of water	Pa	
r'	radial coordinate	m	
r	non-dimensional radial coordinate (r'/a)		
R	universal gas constant	$J\,kg^{-1}\,K^{-1}$	
t	time	s	
V_s	Stefan flow velocity	$m\,s^{-1}$	
α	thermal diffusivity	$m^2\,s^{-1}$	
β	extinction coefficient	m^{-1}	
κ	absorption coefficients	m^{-1}	
ρ	density	$kg\,m^{-3}$	
α_1, α_2	stoichiometric coefficients of two competing reactions		

Subscripts

a	air
char	char content in coal
CO	carbon monoxide
CO_2	carbon dioxide
H_2O	water
H_2	hydrogen
N_2	nitrogen
O_2	oxygen
vol	volatile matter content in coal
i	initial state/species
j	reactions
r	reference state
∞	free stream

Superscripts

g	gas phase
p	particle phase

ics and chemistry of reaction. Several computer codes are available to predict the rate of volatile release and the composition of key species during devolatilization of coal. The codes are based on either constant activation energy model with two competing reaction paths or distributed activation energy model with several simultaneous first order reaction paths of the process of devolatilization.

A couple of works [24–26] pertain to the modeling of pulverized coal combustion in a blowpipe, drop tube and raceway zone of a blast furnace. The models are based on either Eulerian–Lagrangian or Eulerian–Eulerian approach and depend on the empirical values of transport coefficients and coal reactivities at several stages of the physical process. The concept of mixture fraction along with pdf function for interaction of coal combustion with gas phase turbulence has been considered in the models based on Eulerian–Lagrangian approach. The outcome of these models are the predictions of trajectories of burning coal particles, temperature histories in combustion zone and the emission characteristics including the optimization of NO_x emission.

The combustion of a cluster of pulverized coal particle in a combustor is guided by the combustion characteristics of a single coal particle in a surrounding of hot gas. The combustion history and the relative weightage of different physical processes during the combustion of a single coal particle depends on the temperature response of the particle which in turn is guided by the rate of heat transfer from the local gas phase to the particle along with the rate of heterogeneous reaction at the particle surface. Again, the heat transfer from local gas phase depends on the gas phase temperature, which is determined mainly by the rate of homogeneous gas phase reactions. Thereafter, it appears that a comprehensive model of coal particle combustion requires the coupling of chemical reactions at several stages with the transport processes of heat, mass and momentum in the carrier gas phase. However, the work of this nature is hardly found in literature.

Another important aspect which has not yet received much attention is the thermodynamic irreversibilities in the process of coal combustion. The studies on thermodynamic irreversibility find its importance in determining the exergy loss in the process in preserving the quality of energy. Approximately 1/3 of the useful energy of the fuel is destroyed during the combustion processes. Most of the exergy analysis is nowadays conducted on the system level development by evaluating the exergy values and changes of component input and output stream and energy interactions. While this can indeed identify the exergy destruction in a system component, it does not deliver the detailed information about the specific process phenomena, often space and time dependent, which causes the exergy changes or irreversibilities. This type of detailed analysis is invaluable in accelerating the innovative combustion system needed to meet the difficult demands of the coming century. A couple of works [27–37] related with exergy destruction in spray and pulverized coal combustion processes are available in the literature. However the information regarding the intrinsic thermodynamic irreversibilities for single pulverized coal particle combustion is not available in the literature till date.

The present work makes an effort to provide a detailed analysis of exergy destruction (thermodynamic irreversibilities) contributed by different modes of transport processes and chemical reactions for a single pulverized coal particle combustion process.

2. Theoretical formulation

2.1. Physical model

The physical problem deals with the combustion of a single pulverized coal particle in a quiescent medium of air (Fig. 1). Free stream temperature of the medium is considered to be higher than the initial temperature of the particle. The ambient pressure is taken to be the normal atmospheric pressure (101 kN/m^2). The influence of gravity is neglected in consideration of very small diameter of the particle (in the range of 40 to 100 μm) and the thermodynamic equilibrium is assumed to exist at the interface of the particle and the surrounding gas.

A spherical coordinate system (Fig. 1) with the origin attached to the centre of the particle is chosen for the theoretical analysis. Since the influence of gravity is neglected, the present problem is spherico-symmetric in nature. Hence all the conservation equations are one-dimensional in space i.e., function of r' (the radial coordinate in Fig. 1) only.

When a pulverized coal particle is being heated, it undergoes a number of sequential physical processes like (i) moisture evaporation, (ii) devolatilization and (iii) char combustion. Accordingly, the gas phase reveals different physical processes like diffusion of water vapor, gas phase combustion of volatile matter at different steps, and mainly gas phase combustion of carbon monoxide. The sequence of all these processes depends upon the characteristics and the mechanistic models of the physical processes. However, all these processes are guided by the conservation principles of heat, mass and momentum in both the solid and gas phases and by the kinetics of chemical reactions which take place.

2.2. Conservation equations

2.2.1. Gas phase

2.2.1.1. Conservation of mass and momentum. The blowing at the particle surface, due to evaporation of moisture, release of volatile gases during devolatilization, and release of carbon monoxide gases during char combustion induces a purely radial flow in the gas phase. The continuity equation can be written, under the situation, as

$$\frac{1}{r^2}\frac{\partial}{\partial r}\left(r^2 V_r\right) = 0 \tag{1}$$

or,

$$V_r = \frac{V_s}{r^2} \tag{2}$$

where V_s is the blowing or Stefan flow velocity at the surface ($r = 1$).

Conservation of momentum is not needed to be considered separately since for small flow velocity at the particle surface, the pressure in surrounding gas phase is considered to be uniform and equals to the prescribed ambient pressure.

2.2.1.2. Conservation of energy.

$$\frac{\partial T^g}{\partial t} + \frac{1}{a}V_r\frac{\partial T^g}{\partial r} = \alpha^g\frac{1}{a^2}\left[\frac{\partial^2 T^g}{\partial r^2} + \frac{2}{r}\frac{\partial T^g}{\partial r}\right] + \kappa\left(\frac{G - 4\sigma T^{g4}}{\rho^g c_p^g}\right) + \frac{S_e^g}{\rho^g c_p^g} \tag{3}$$

The second term in the right-hand side of Eq. (3) arises due to the consideration of radiation in gas phase following a simplified model as described below. The term S_e^g in the right-hand side of Eq. (3) is the sum of all the source terms due to gas phase combustion.

2.2.1.3. Radiation model. The radiative energy exchange is evaluated within the gas phase assuming the gas phase to be a gray, absorbing and emitting medium. The radiative transfer equation is solved following a first order moment method which reduces the integro-differential equation of radiative energy transfer into a differential equation. The differential approximation for radiative transfer [38] yields

$$q_R = -\frac{1}{3\beta}\nabla G \tag{4}$$

And the equation for radiative transfer becomes

$$\nabla^2 G = 3\beta\kappa\left[G - 4\sigma T^{g4}\right] \tag{5}$$

For a non-scattering gas, $\beta = \kappa$.

Then the radiative transfer equation can be written in a form as

$$\frac{\mathrm{d}^2 G}{\mathrm{d}r^2} + \frac{2}{r}\frac{\mathrm{d}G}{\mathrm{d}r} = 3\kappa^2 a^2\left(G - 4\sigma T^{g4}\right) \tag{6}$$

For the solution of radiative transfer equation (6), Marshak boundary condition has been used. This leads to the following expression of irradiation G, as the boundary condition as (8)

$$\frac{2}{3}(1+\rho)\frac{\mathrm{d}G}{\mathrm{d}r} = a\kappa\left[(1-\rho)G - 4\varepsilon\sigma T^4\right] \quad \text{for } r = 1 \tag{7}$$

$$\frac{2}{3}(1+\rho)\frac{\mathrm{d}G}{\mathrm{d}r} = -a\kappa\left[(1-\rho)G - 4\varepsilon\sigma T^4\right] \quad \text{for } r = \infty \tag{8}$$

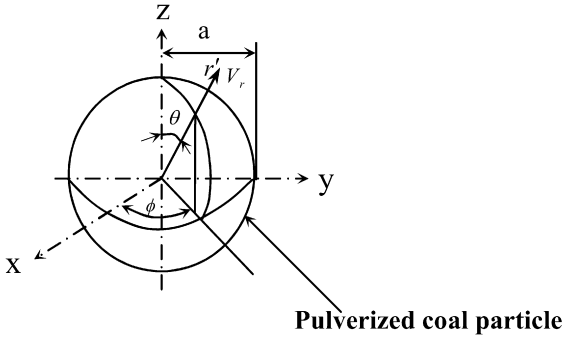

Fig. 1. Physical model and system coordinates.

also,

$$\rho + \tau + \varepsilon = 1$$

where ρ, τ and ε are the reflectivity, transmissivity and emissivity of the corresponding boundary surfaces respectively.

2.2.1.4. Species conservation equation.

$$\frac{\partial C_i^g}{\partial t} + \frac{1}{a} V_r \frac{\partial C_i^g}{\partial r} = \frac{D^g}{a^2}\left[\frac{\partial^2 C_i^g}{\partial r^2} + \frac{2}{r}\frac{\partial C_i^g}{\partial r}\right] + \frac{S_{c_i}^g}{\rho^g} \tag{9}$$

The subscript 'i' in Eq. (9) represents the identity of a species. The term $S_{c_i}^g$ in the right-hand side of Eq. (9) represents the sum of all the source terms for the species 'i' due to gas phase chemical reactions. The species conservation equation is solved for water vapor, volatile matter, carbon monoxide, hydrogen, carbon dioxide and oxygen, while nitrogen concentration is obtained by difference.

2.2.2. Particle phase

2.2.2.1. Conservation of energy.

$$m^p c_p^p \frac{\mathrm{d}T^p}{\mathrm{d}t} = 4\pi K^g a \left.\frac{\mathrm{d}T}{\mathrm{d}r}\right|_{r=1} + S_e^p \tag{10}$$

The last term S_e^p in the right-hand side of Eq. (10) represents the source term as arising out of different situations.

2.2.3. Mass depletion rate of coal particle

The rate of depletion of coal particle mass at any instant can be written as

$$\frac{\mathrm{d}m^p}{\mathrm{d}t} = -\left(\frac{\mathrm{d}m_{\mathrm{H_2O}}}{\mathrm{d}t} + \frac{\mathrm{d}m_{\mathrm{vol}}}{\mathrm{d}t} + \frac{\mathrm{d}m_{\mathrm{char}}}{\mathrm{d}t}\right) \tag{11}$$

where $\frac{\mathrm{d}m_{\mathrm{H_2O}}}{\mathrm{d}t}$, mass depletion due to evaporation of moisture, $\frac{\mathrm{d}m_{\mathrm{vol}}}{\mathrm{d}t}$, mass loss due to pyrolysis reaction and $\frac{\mathrm{d}m_{\mathrm{char}}}{\mathrm{d}t}$, mass consumed during char reaction at the surface.

2.2.4. Model of moisture evaporation

The process of moisture evaporation takes place mostly in the initial part of the particle heating. It is assumed that water inside the coal particle comes out continuously at the surface and makes the surface wet in the form of a thin water film from which evaporation of water takes place into the hot surrounding air. The radial velocity of Stefan flow due to evaporation is found out by considering the gas liquid interphase to be impermeable to all non-evaporating species, as

$$V_s = \left(\frac{D^g}{a}\right)\frac{(-\frac{\partial C_{\mathrm{H_2O}}}{\partial r}|_{r=1})}{(1 - C_{\mathrm{H_2O},s})} \tag{12}$$

The mass fraction of water vapor at the interphase can be written in consideration of thermodynamic equilibrium and the ideal gas phase behavior of the surrounding medium as

$$C_{\mathrm{H_2O},s} = \frac{1}{1 + (\frac{M_a}{M_{\mathrm{H_2O}}})(\frac{P_\infty}{P_v} - 1)} \tag{13}$$

The rate of evaporation can be expressed as

$$\frac{\mathrm{d}m_{\mathrm{H_2O}}}{\mathrm{d}t} = 4\pi a^2 \rho^g V_s \tag{14}$$

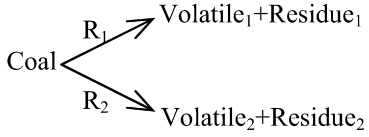

Fig. 2. Two step kinetic model for pyrolysis reaction.

During the moisture evaporation period,

$$S_e^p\big(\text{in Eq. (10)}\big) = -\frac{\mathrm{d}m_{\mathrm{H_2O}}}{\mathrm{d}t}\Delta H_{\mathrm{vap}} \tag{15}$$

2.2.5. Model of devolatilization

The pyrolysis reaction inside the coal particle and the subsequent release of volatile gases from the coal surface take place at an extremely slow rate at lower temperature usually less than 500 K. However as the particle temperature increases, the rate of pyrolysis reaction increases and the process of devolatilization becomes prominent.

The rate of release of volatile gases $\frac{\mathrm{d}m_{\mathrm{vol}}}{\mathrm{d}t}$ is determined following the well established Kobayashi's two competing-reaction kinetic model [39] of pyrolysis process as, as shown in Fig. 2.

Therefore,

$$\frac{\mathrm{d}m_{\mathrm{vol}}}{\mathrm{d}t} = \left[m_i^p(\alpha_1 R_1 + \alpha_2 R_2)\exp\left(-\int_0^t (R_1 + R_2)\,\mathrm{d}t\right)\right] \tag{16}$$

where

$$R_1 = A_{v1}\exp\left(-\frac{E_{v1}}{RT^p}\right) \tag{17}$$

$$R_2 = A_{v2}\exp\left(-\frac{E_{v2}}{RT^p}\right) \tag{18}$$

2.2.5.1. Gas phase combustion of volatile matter. The gaseous volatile matter has been represented as a generic hydrocarbon C_nH_m where the values of n and m are found out from the mass composition (ultimate analysis) of coal. The combustion of C_nH_m has been considered by three step irreversible reactions as follows.

Reactions

$$C_nH_m + \frac{1}{2}nO_2 \xrightarrow{\dot{\omega}_1} \frac{1}{2}mH_2 + nCO \tag{19}$$

$$CO + \frac{1}{2}O_2 \xrightarrow{\dot{\omega}_2} CO_2 \tag{20}$$

$$H_2 + \frac{1}{2}O_2 \xrightarrow{\dot{\omega}_3} H_2O \tag{21}$$

The rate constants $\dot{\omega}_1$, $\dot{\omega}_2$, and $\dot{\omega}_3$ for reactions (19), (20) and (21) are given by

$$\dot{\omega}_1 = A_1\big(T^g\big)p^{0.3}\left(\frac{C_{C_nH_m}\rho^g}{M_{C_nH_m}}\right)^{a1}\left(\frac{C_{O_2}\rho^g}{M_{O_2}}\right)^{b1}\exp\left(-\frac{E_1}{RT^g}\right) \tag{22}$$

$$\dot{\omega}_2 = A_2\left(\frac{C_{\mathrm{CO}}\rho^g}{M_{\mathrm{CO}}}\right)^{a2}\left(\frac{C_{\mathrm{O_2}}\rho^g}{M_{\mathrm{O_2}}}\right)^{b2}\left(\frac{C_{\mathrm{H_2O}}\rho^g}{M_{\mathrm{H_2O}}}\right)^{c2}\exp\left(-\frac{E_2}{RT^g}\right) \tag{23}$$

$$\dot{\omega}_3 = A_3\left(\frac{C_{\mathrm{H_2}}\rho^g}{M_{\mathrm{H_2}}}\right)^{a3}\left(\frac{C_{\mathrm{O_2}}\rho^g}{M_{\mathrm{O_2}}}\right)^{b3}\exp\left(-\frac{E_3}{RT^g}\right) \tag{24}$$

2.2.5.2. Gas phase source terms. The energy source term S_e^g in Eq. (3) under the situation is written as

$$S_e^g = S_e^{\mathrm{C}_n\mathrm{H}_m} + S_e^{\mathrm{CO}} + S_e^{\mathrm{H_2}} \tag{25}$$

where

$$S_e^{\mathrm{C}_n\mathrm{H}_m} = \dot{\omega}_1 M_{\mathrm{C}_n\mathrm{H}_m}\Delta H_{\mathrm{C}_n\mathrm{H}_m} \tag{26}$$

$$S_e^{\mathrm{CO}} = \dot{\omega}_2 M_{\mathrm{CO}}\Delta H_{\mathrm{CO}} \tag{27}$$

$$S_e^{\mathrm{H_2}} = \dot{\omega}_3 M_{\mathrm{H_2}}\Delta H_{\mathrm{H_2}} \tag{28}$$

where $\Delta H_{\mathrm{C}_n\mathrm{H}_m}$, ΔH_{CO} and $\Delta H_{\mathrm{H_2}}$ are the enthalpy of combustion reactions in Eqs. (19), (20) and (21) respectively.

The mass source terms $S_{c_i}^g$ in Eq. (9) for different species is given by the following expressions

$$S_c^{\mathrm{C}_n\mathrm{H}_m} = \dot{\omega}_1 M_{\mathrm{C}_n\mathrm{H}_m} \tag{29}$$

$$S_c^{\mathrm{CO}} = (n\dot{\omega}_1 - \dot{\omega}_2)M_{\mathrm{CO}} \tag{30}$$

$$S_c^{H_2} = \left(\frac{1}{2}m\dot{\omega}_1 - \dot{\omega}_3\right)M_{\mathrm{H_2}} \tag{31}$$

$$S_c^{\mathrm{CO_2}} = \dot{\omega}_2 M_{\mathrm{CO_2}} \tag{32}$$

$$S_c^{\mathrm{H_2O}} = \dot{\omega}_3 M_{\mathrm{H_2O}} \tag{33}$$

$$S_c^{\mathrm{O_2}} = -\left[\frac{1}{2}n\dot{\omega}_1 + \frac{1}{2}\dot{\omega}_2 + \frac{1}{2}\dot{\omega}_3\right]M_{\mathrm{O_2}} \tag{34}$$

2.2.5.3. Particle phase source term. The particle source term S_e^p in Eq. (10) due to the pyrolysis reaction inside the coal particle can be written as

$$S_e^p = -\frac{\mathrm{d}m_{\mathrm{vol}}}{\mathrm{d}t}\Delta H_{\mathrm{vol}} \tag{35}$$

2.2.6. Model of char combustion

Char combustion is considered to take place only at the coal surface in the present model. The one step irreversible chemical reaction in this regard is considered to be

$$\mathrm{C} + \frac{1}{2}\mathrm{O_2} = \mathrm{CO} \tag{36}$$

The CO thus produced is converted to CO_2 by the gas phase chemical reaction as shown in Eq. (20).

The rate of char combustion reaction is written according to models of Baum and Street [40] and Field [41],

$$\frac{\mathrm{d}m_{\mathrm{char}}}{\mathrm{d}t} = \pi d^{p2}\rho^g RT^g\left(\frac{C_{\mathrm{O_2}}}{M_{\mathrm{O_2}}}\right)\frac{R_C R_D}{R_C + R_D} \tag{37}$$

$$R_D = C_1\frac{[(T^P + T^g)/2]^{0.75}}{d^p} \tag{38}$$

$$R_C = A_c\exp\left(-\frac{E_C}{RT^P}\right) \tag{39}$$

and corresponding CO production rate will be

$$\frac{\mathrm{d}m_{\mathrm{CO}}}{\mathrm{d}t} = 2.33\frac{\mathrm{d}m_{\mathrm{char}}}{\mathrm{d}t} \tag{40}$$

During the period of devolatilization and char combustion, the Stefan flow velocity at particle surface is given by

$$V_s = \frac{\mathrm{d}m_{\mathrm{vol}}}{\mathrm{d}t}\left(\frac{1}{4\pi\rho^g a^2}\right) + \frac{\mathrm{d}m_{\mathrm{CO}}}{\mathrm{d}t}\left(\frac{1}{4\pi\rho^g a^2}\right) \tag{41}$$

However, during the initial period, the term $\frac{\mathrm{d}m_{\mathrm{vol}}}{\mathrm{d}t}$ dominates, while during the later stage $\frac{\mathrm{d}m_{\mathrm{CO}}}{\mathrm{d}t}$ will be the dominating one in determine the values of V_s.

2.2.6.1. Particle phase source term. The particle source term S_e^p in Eq. (10) due to the char reaction at the coal surface can be written as

$$S_e^p = \frac{\mathrm{d}m_{\mathrm{char}}}{\mathrm{d}t}\Delta H_{\mathrm{char}} \tag{42}$$

2.3. Initial and boundary conditions

The initial and boundary conditions for the solution of Eqs. (3), (9) and (10) are as follows.

2.3.1. Initial conditions

At

$t = 0$

$$(r = 1)\quad T^g = T^p \tag{43}$$

$$(r > 1)\quad T^g = T_\infty,\ C_i = 0.0$$

(for all species except for O_2 and N_2)

$$C_{\mathrm{O_2}} = 0.232,\ C_{\mathrm{N_2}} = 0.768 \tag{44}$$

2.3.2. Boundary conditions

At solid–gas interface:

$(r = 1)$

$$(t > 0)\quad T^g = T^p \tag{45}$$

The boundary conditions for concentrations of different species at solid–gas interface ($r = 1$) cannot be written into a general form. The boundary conditions for different species are described below.

- Water vapor:

$$C_{\mathrm{H_2O}} = C_{\mathrm{H_2O},s} \tag{46}$$

where $C_{\mathrm{H_2O},s}$ is determined from Eq. (13).

- Volatile matter:

$$\frac{\partial C_{\mathrm{C}_n\mathrm{H}_m}}{\partial r} = \left(\frac{a}{D^g}\right)C_{\mathrm{C}_n\mathrm{H}_m}V_s - \frac{\mathrm{d}m_{\mathrm{vol}}}{\mathrm{d}t}\left(\frac{1}{4\pi D^g\rho^g a}\right) \tag{47}$$

- Carbon monoxide:

$$\frac{\partial C_{\mathrm{CO}}}{\partial r} = \left(\frac{a}{D^g}\right)C_{\mathrm{CO}}V_s - \frac{\mathrm{d}m_{\mathrm{CO}}}{\mathrm{d}t}\left(\frac{1}{4\pi D^g\rho^g a}\right) \tag{48}$$

- All other species:

$$\frac{\partial C_i}{\partial r} = \left(\frac{a}{D^g}\right) C_i V_s \tag{49}$$

Eqs. (47) and (48) are obtained by equating the rate of release of volatile matter and carbon monoxide from the coal surface with combined convection and diffusion of volatile matter and carbon monoxide species respectively. Eq. (49) originates from the impermeability condition of the species concerned at the coal surface.

At free stream: $(r \to \infty)$
$(t > 0)$

$$T^g = T_\infty \tag{50}$$

$$\frac{\partial C_i}{\partial r} = 0 \quad \text{(for all species except } O_2\text{)}$$

$$C_{O_2} = 0.232 \tag{51}$$

2.4. Determination of process irreversibilities

The thermodynamic irreversibility in the entire process of coal combustion is due to the effects of heat, mass and momentum transport and the chemical reactions in the gas phase. It is characterized quantitatively by the rate of entropy production, evaluated from the principle of entropy conservation. The local entropy generation rate per unit volume in a continuous field involving heat, mass and momentum transfer of an incompressible Newtonian fluid in presence of a chemical reaction but without body force effects, can be written following the general formulation of Bejan [42], Krickwood and Crawford [43] and Hirschfelder et al. [44] as

$$\dot{e} = \underbrace{\frac{\Delta : \sigma}{T}}_{\dot{e}_1} + \underbrace{\frac{(-J_q.\nabla T)}{T^2}}_{\dot{e}_2} + \underbrace{\frac{\sum(-J_m.\nabla\mu_c)}{T}}_{\dot{e}_3} + \underbrace{\frac{\sum(-\bar{s}_i J_m.\nabla T)}{T}}_{\dot{e}_4} + \underbrace{\frac{\sum\sum\lambda_i\mu_{ci}|\dot{\omega}|}{T}}_{\dot{e}_5} \tag{52}$$

where Δ and σ $(= \mu\Delta)$ are the rates of strain and stress tensors respectively, and J_q, and J_m are respectively the heat and mole fluxes per unit surface area.

The first term in Eq. (52) is due to fluid friction, the second term is due to heat conduction, the third term pertains to mass transfer, the fourth term arises from the coupling between heat and mass transfer and the fifth term is due to chemical reaction. The flow velocity in the gas phase is very small compared to the local acoustic speed and hence the effect of viscous dissipation, i.e., the first term of Eq. (52), is neglected.

In consideration of the gas phase to be a mixture of ideal gases, the chemical potential of any species can be written as

$$\mu_{c_i}(T, P) = \mu^0_{c_i}(T) + RT\ln\left(\frac{P_i}{P}\right) \tag{53}$$

where P is the total pressure, P_i and $\mu^0_{c_i}(T)$ are the partial pressure and the standard state chemical potential, respectively of species i. Hence we can write,

$$\nabla\mu_{c_i} = \frac{RT}{P_i}\nabla P_i = \frac{RT}{C_i}\nabla C_i \tag{54}$$

with the help of Eq. (54), the third term of Eq. (52) can be written as

$$\dot{e}_3 = \frac{D^g\rho^g R}{M_i C_i}(\nabla C_i.\nabla C_i) \tag{55}$$

The second, third and fourth terms of Eq. (52) can be written in a spherical coordinates system for the present case as

$$\dot{e}_2 = \frac{K^g}{T^{g2}}\left(\frac{\partial T^g}{\partial r'}\right)^2 \tag{56}$$

$$\dot{e}_3 = \frac{D^g\rho^g R}{M_i C_i}\left(\frac{\partial C_i}{\partial r'}\right)^2 \tag{57}$$

$$\dot{e}_4 = \frac{\bar{s}_i D^g\rho^g}{T^g M_i}\left[\left(\frac{\partial C_i}{\partial r'}\right)\left(\frac{\partial T^g}{\partial r'}\right)\right] \tag{58}$$

Partial molal entropy $\bar{s}_i$ appearing in Eq. (58) can be expressed as

$$\bar{s}_i = -\left(\frac{\partial\mu_c}{\partial T}\right)_{P,n_j\ (j\neq i)} = -R\ln\left(\frac{P_i}{P_r}\right) + \int_{T_r}^{T^g}\frac{c_{p_i}M_i}{T^g}\,\mathrm{d}T^g + \bar{s}_{i_r} \tag{59}$$

where $\bar{s}_{i_r}$ is the partial molal entropy of different species at a reference pressure and temperature P_r and T_r respectively. The fifth term of Eq. (52) representing the entropy generation rate per unit volume due to chemical reaction can be written as

$$\dot{e}_5 = \frac{\sum_{j=1}^m\sum_{i=1}^n\lambda_i\mu_{c_i}\dot{\omega}_j}{T^g} \tag{60}$$

where $\dot{\omega}_j$ is the reaction rate of a jth reaction and μ_{c_i}, λ_i are the chemical potential and stoichiometric coefficients respectively for species taking part in the reactions. With the help of Eq. (53), the chemical potential of a species in a mixture can be written in a form as

$$\mu_{c_i} = \int_{T_r}^{T^g} c_{p_i}M_i\,\mathrm{d}T^g - T^g\int_{T_r}^{T^g}\frac{c_{p_i}M_i}{T^g}\,\mathrm{d}T^g + h_i - T^g s_i + RT^g\ln\left(\frac{P_i}{P_r}\right) \tag{61}$$

where h_i and s_i are the molal enthalpy and entropy respectively at a reference state of pressure and temperature P_r and T_r. The total entropy generation rate $\dot{E}$ at any instant is found out by integrating the local entropy generation rate per unit volume over the spatial domain of the transport processes as,

$$\dot{E} = 4\pi a^3\int_1^{r_\infty}\dot{e}r^2\,\mathrm{d}r \tag{62}$$

Table 1
Different input parameters for present study

Free stream air temperature, T_∞	1400 K, 1600 K, 1800 K								
Initial particle diameter, d_i^p	60 μm, 80 μm, 100 μm								
Initial particle temperature, T_i^p	300 K								
	Proximate analysis (%)				Ultimate analysis (dry %)				
Composition of coal particle	Volatile matter	Fixed carbon	Moisture	Ash	C	H	N	S	O
	10.0	70.6	1.3	18.1	73.2	3.1	0.9	0.9	3.8
	28.0	62.0	2.0	8.0	78.5	5.45	2.5	0.8	4.6
	40.0	47.6	3.7	8.7	70.2	5.7	1.4	0.5	13.4
Kinetic parameters	Kobayashi model (Eqs. (17), (18))			$A_{v1} = 2.0 \times 10^5$, $E_{v1} = 1.046 \times 10^8$ (J kmol^{-1}) $A_{v2} = 1.3 \times 10^7$, $E_{v2} = 1.67 \times 10^8$ (J kmol^{-1})					
	Combustion of volatile matter (Eqs. (22)–(24))			$A_1 = 59.8$, $E_1 = 1.0143 \times 10^8$ (J kmol^{-1}) $A_2 = 1.0 \times 10^{14.6}$, $E_2 = 4.0 \times 10^7$ (J kmol^{-1}) $A_3 = 1.0 \times 10^{13.52}$, $E_3 = 4.1 \times 10^7$ (J kmol^{-1})					
	Baum and Street model (Eqs. (38), (39))			$C_1 = 5 \times 10^{-12}$, $A_c = 0.002$, $E_c = 7.9 \times 10^7$ (J kmol^{-1})					

where

$$\dot{e} = \dot{e}_1 + \dot{e}_2 + \dot{e}_3 + \dot{e}_4 + \dot{e}_5$$

The instantaneous rate of irreversibilities can be expressed as

$$\dot{I} = T_r \dot{E} \tag{63}$$

Total amount of irreversibilities during the entire process of coal combustion can be written as

$$I = \int_0^{t_l} \dot{I}\, \mathrm{d}t \tag{64}$$

where t_l, the upper limit of integration, is the coal burn out time.

3. Method of solution

The gas phase conservation equations (2), (3), (9) and the particle phase energy equation (10) were solved numerically with the aid of finite difference method. For the solution of equations in the gas phase, the radial coordinate r was transformed to $r = e^z$ for the use of a constant step size for z to obtain a relatively denser mesh near the particle surface. All the time dependent conservation equations were solved using explicit scheme. However, the radiative transfer equation was solved by an implicit scheme, the finite difference analogue of which resulted in a set of linear equations having a tri-diagonal coefficient matrix and was solved using Thoma's algorithm. The space derivatives in the conservation equations were discretised by central difference scheme for the diffusion terms and by a full second upwind scheme for the advection terms. Central difference scheme was also employed for the space derivatives in radiative transfer equations.

3.1. Grid specification and time step

A mesh size of $\Delta z = 0.05$ and $z_\alpha = 4.0$ (corresponding to a value of $r_\alpha = 54.6$) for gas phase was chosen for numerical computation. The test for grid independence and the free stream distance was made to ensure that a mesh size finer than the stated one and a free stream distance z_α beyond 4.0 produced insignificant changes (below 3%) in the values of temperature and concentration field. The choice of time increment Δt for the explicit advancement of the variables was made to ensure stability in the computation in accordance with the criteria of cell transit time of fluid due to convection and diffusion respectively. A time step of $\Delta t = 0.0001$ was used for the present purpose. Air was taken as the free stream ambience. Gas phase was considered to be a mixture of ideal gases and its thermophysical properties were assumed to be spatially constant but updated with time. The property values were evaluated using 2/3–1/3 rules for reference temperature in the gas phase (reference temperature equaled the sum of 2/3rd value at particle surface and 1/3rd value at free stream). The property values for gas phase and particle phase were calculated from standard literatures [36,45,46]. The different input parameters taken for the present study is shown in Table 1.

The dominant radiation intensity in the carrier phase was due to CO_2, H_2O and CO. In the light of the assumption of gray gas radiation model, the absorption coefficient κ in Eq. (3) was replaced by Planck's mean absorption coefficient κ_P. The local value of κ_P was computed as,

$$\kappa_P = C_{\mathrm{H_2O}} \kappa_{P_{\mathrm{H_2O}}}(T) + C_{\mathrm{CO_2}} \kappa_{P_{\mathrm{CO_2}}}(T) + C_{\mathrm{CO}} \kappa_{P_{\mathrm{CO}}}(T)$$

The values of $\kappa_P(T)$ as a function of temperature for CO_2, H_2O and CO were taken from standard literature [47].

4. Results and discussion

4.1. Temperature and mass histories of coal particle

Figs. 3(a) and (b) show the influence of free stream temperature on the particle temperature-time history and the mass burning rate of the particle respectively. The portion 'AB' of the curves in Figs. 3(a) and (b) corresponds to the initial process of particle heating and its moisture evaporation in a surrounding of hot air. During this part, there is a negligible release of volatile matter depicting almost a constant mass of the particle (the portion 'AB' in Fig. 3(b)). The steep temperature-time

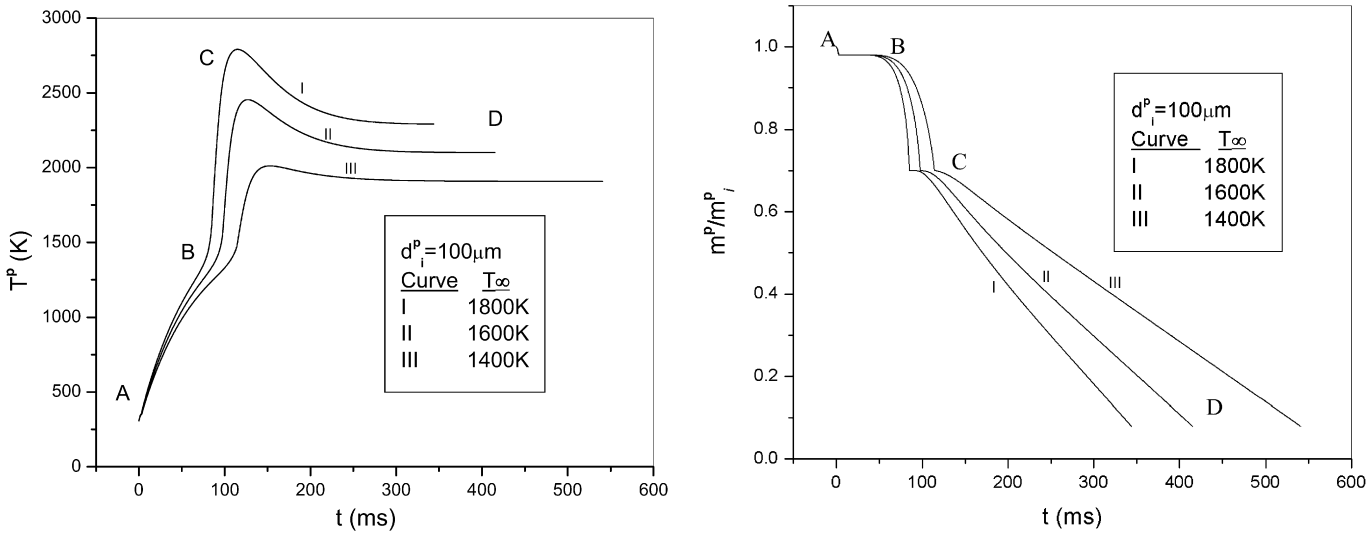

(a) (b)

Fig. 3. (a) Temporal histories of particle temperature for different values of free stream temperature. (b) Temporal histories of particle mass for different values of free stream temperature.

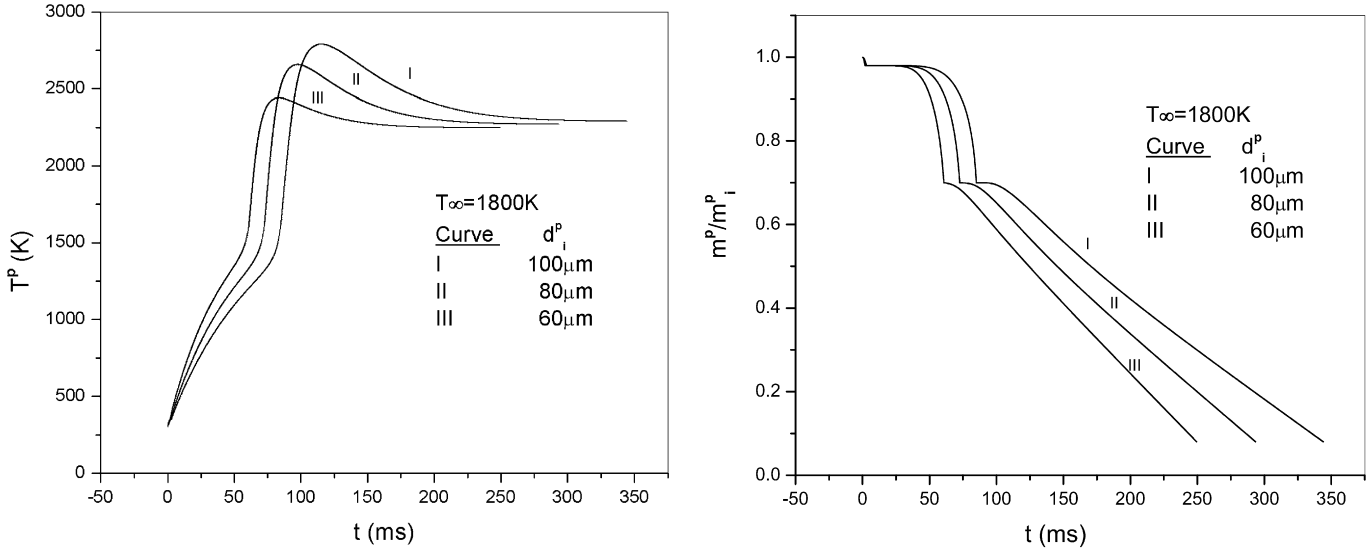

(a) (b)

Fig. 4. (a) Temporal histories of particle temperature for different values of initial particle diameter. (b) Temporal histories of particle mass for different values of initial particle diameter.

response of the particle and the faster rate in the reduction of particle mass during the volatile matter release and combustion in the gas phase are shown by the portion "BC" of the curves in Figs. 3(a) and (b) respectively. It is observed from Fig. 3(a) that the particle reaches a maximum temperature (the point "C" on the curve) and then, after a certain decrease, it attains almost a constant temperature during the rest part ("CD") of its burnout. This can be physically explained by the fact that near the completion of the process of volatile combustion, there takes place the combustion of char at the coal surface which is also responsible for the heating of the coal particle. During this part of the process, the coal mass is reduced at a steady rate as shown by the portion 'CD' in curve of Fig. 3(b).

It is also observed that an increase in free stream temperature results in a steeper temperature rise of the particle and increases the maximum temperature and the steady state temperature attained by the particle. Again, with an increase in free stream temperature, the mass burning rate of the particle increases and it results in a lower burnout time as shown in Fig. 3(b).

Fig. 4(a) shows the influence of initial particle diameter, d_i^p, on the temporal history of particle temperature, T^p. It is observed that with an increase in initial particle diameter, the temperature response of the particle in its initial heating period becomes relatively slow. This is obvious since the rate of heat transfer to the particle per unit mass is an inverse function of its diameter. However, the bigger particle releases more

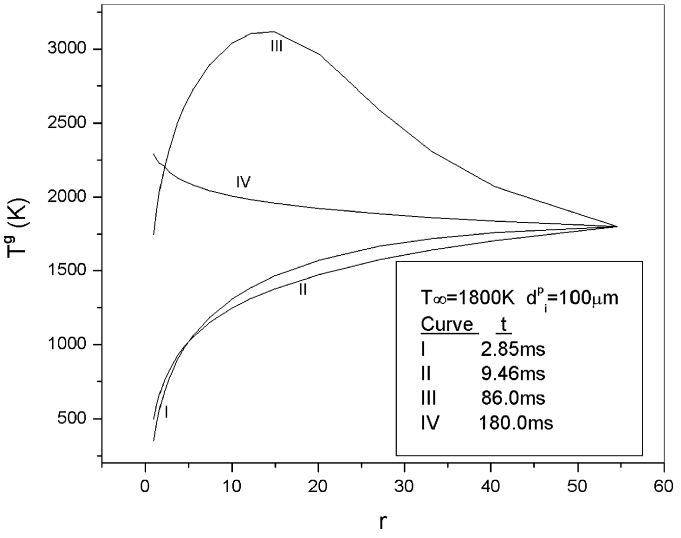

Fig. 5. Gas phase temperature distribution at different instants of time.

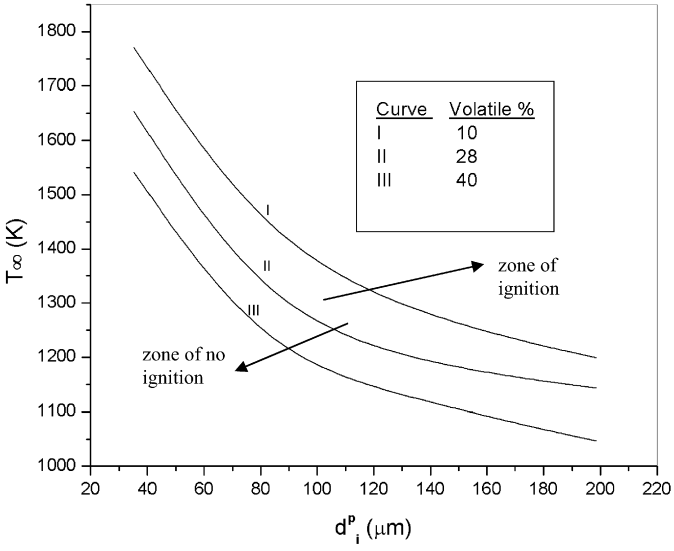

Fig. 6. Influence of volatile matter on ignition characteristics of coal particle.

volatile gases which in the process of combustion result in a higher temperature of the local gas phase. This causes the particle to be heated to a higher temperature. Therefore it is observed in Fig. 4(a) that the maximum temperature attained by a particle increases with an increase in its initial diameter. It is also observed that the initial particle diameter has almost negligible influence on the steady state temperature attained by the particle.

Fig. 4(b) shows that with a decrease in initial particle diameter, the mass burning rate of the particle is increased resulting in a lower burnout time. This is because the char burning rate, which is the rate determining step of coal burning process, is an inverse function of particle diameter.

The Fig. 5 shows the spatial distribution of gas phase temperature T^g at different instants of time. The curves I and II correspond to the period of particle heating without considerable release of volatile matter. Therefore, the gas phase temperature increases monotonically from the coal surface to the free stream. The maximum gas phase temperature during this period is the free stream temperature while the coal surface temperature remains at a relatively low value. The curve III corresponds to an instant of intense gas phase combustion of volatile matter and the beginning of char combustion at coal surface. Because of this, the temperature in the gas phase near the coal surface shoots up to a high value beyond the free stream temperature and then gradually decreases to that of the free stream. During this regime, the surface temperature of the coal particle is relatively high. The curve IV corresponds to an instant when the gas phase combustion of volatile matter is almost complete due to the lack of any volatile gas available in the surrounding. The intense char combustion is initiated at this instant and hence the coal surface temperature is increased to a very high value. Therefore, the gas phase temperature distribution during this period shows a monotonically decreasing trend from a maximum value at the coal surface to the free stream temperature.

4.2. Ignition characteristics

Fig. 6 shows the influence of the amount of volatile matter in a coal particle on its ignition characteristics. Ignition is associated mathematically with the value of $\frac{\partial^2 T^g}{\partial t^2} = 0$, where the temperature time derivative switches from an increasing trend to a decreasing one. The curves in Fig. 6 depict the demarcation lines between possible spontaneously ignitable states to the right from the non-ignitable states to its left. It is observed that for a coal particle of given initial diameter, there is a minimum value of T_∞ below which spontaneous ignition is not possible or, other way, for a given value of T_∞, there is a minimum particle diameter d_i^p below which ignition is not possible.

It is also observed that with an increase in the volatile matter the coal particle becomes more conducive for a spontaneous ignition in a surrounding of hot gas. This means that the threshold free stream temperature for a given particle diameter or the threshold particle diameter for a given free stream temperature decreases with an increase in the volatile matter contained in the coal particle.

4.3. Thermodynamic irreversibility

Figs. 7(a) and (b) show the temporal histories of the rates of thermodynamic irreversibilities associated with the process of pulverized coal combustion at different free stream temperatures and for different values of initial particle diameter. There is a gradual decrease in irreversibility rate during the initial period of particle heating. This is obvious in any transport process since the potential gradient and corresponding flux are maximum at the start of the process and goes on decreasing while the process takes place. The irreversibility during this period arises solely due to conduction of heat through gas phase. The interesting feature to be observed from Figs. 7(a) and (b) is that, after a certain time, the rate of irreversibility shoots up to a high value very fast which is followed immediately by a drastic reduction. Thereafter, the rate of irreversibility follows a

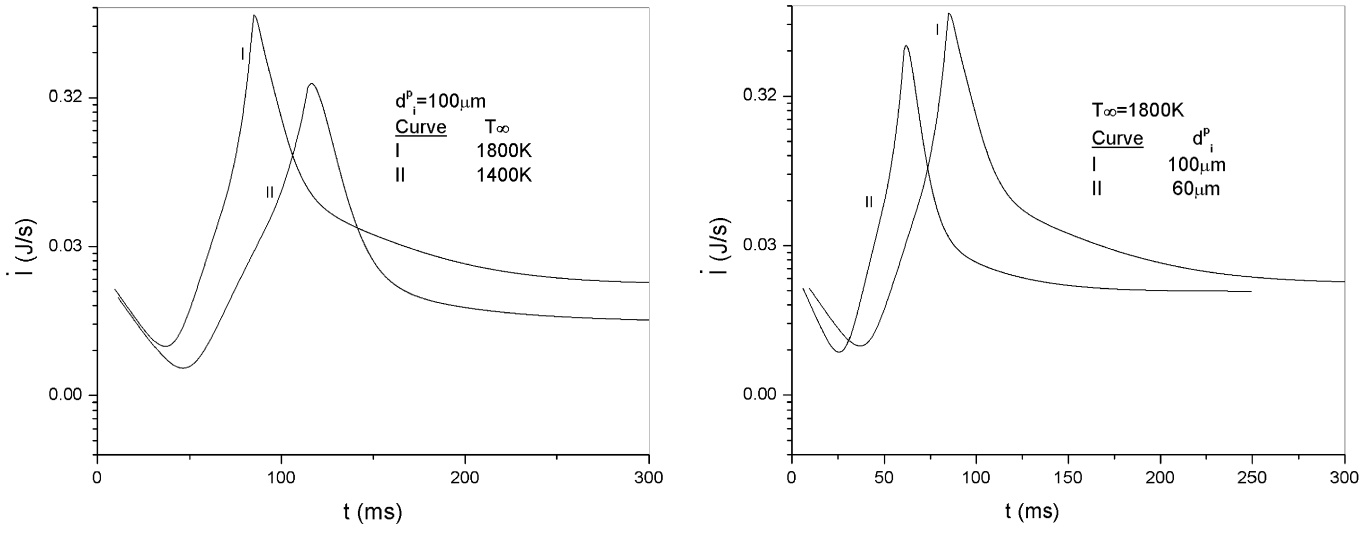

Fig. 7. (a) Temporal histories of irreversibility rate for different values of free stream temperature. (b) Temporal histories of irreversibility rate for different values of initial particle diameter.

Table 2
Comparisons of thermodynamic irreversibilities due to different modes of transport process and chemical reactions in course of combustion of a coal particle

Input parameters		Entropy generation, I (mJ)				
d_i^p	T_∞	Heat conduction	Mass transfer	Coupling of heat and mass transfer	Chemical reaction	Total
	1800 K	4.1367	2.71	8.90	7.4396	23.186
100 μm	1600 K	2.745	2.841	6.522	7.091	19.229
	1400 K	1.392	2.969	3.5627	5.5826	13.506
100 μm		4.1367	2.71	8.90	7.4396	23.186
80 μm	1800 K	3.1483	2.761	7.477	7.0707	20.457
60 μm		2.0996	2.8579	5.6303	6.53	17.1178

gradually decreasing trend to an almost constant value up to the burn out time of the coal particle. This trend of variation in irreversibility rate with time can be attributed to the phenomenon of ignition accompanied by a steep rise in gas phase temperature. The rise in gas phase temperature depicting the onset of combustion causes the rate of entropy generation due to chemical reaction to attain a peak value, resulting in a steep rise in the total rate of generation of entropy. The immediate reduction in irreversibility $\dot{I}$, can be explained in terms of the fact that a first rate of chemical reaction of volatile gases depletes the fuel and oxygen concentration immediately to very low value and thus reduces the rate of entropy generation due to chemical reaction. A further gradual reduction in the irreversibility rate may attribute to a reduction in the temperature and species concentration gradient in the gas phase. However, during the later stage of coal combustion, the chemical reaction of carbon monoxide persists in the gas phase because of the diffusion of carbon monoxide from the coal surface. This counterweighs any further reduction in the irreversibility rate and makes it to be constant during the later part of the coal burning.

An increase in free stream temperature T_∞, decreases the ignition time lag of a coal particle of given diameter and therefore causes the maximum gas phase temperature and the associated rate of irreversibility to shoot up early to a higher value (Fig. 7(a)).

An increase in particle diameter, causes a delay in the ignition of coal particle and results in the same way a delay for the irreversibility rate to shoot up (Fig. 7(b)). However, the maximum value of the irreversibility rate increases with an increase in the particle diameter. This is because of an increase in maximum gas phase temperature with the particle diameter.

Table 2 shows the relative weightage of thermodynamic irreversibilities contributed by different modes of transport processes and chemical reactions. It is observed that under all situations the irreversibility due to coupling of heat and mass transfer and chemical reactions are the dominating ones.

5. Conclusions

A numerical model of the transport processes and associated thermodynamic irreversibilities in the combustion of a single pulverized coal particle has been developed to recognize the influences of coal particle diameter, coal composition and the free stream gas phase temperature on ignition, combustion and irreversibility characteristics of a burning coal particle. The major observations from the model are follows

- An increase in free stream temperature results in a steeper temperature rise of the particle and increases the maximum temperature and the steady state temperature attained by the particle and decreases its lifetime.
- An increase in particle diameter results in a relatively slower temperature-time response of the particle but a higher value of the maximum temperature attained by it. The steady state temperature of the particle is almost uninfluenced by the particle diameter.
- For a given value of free stream gas phase temperature, there is a minimum particle diameter below which the spontaneous ignition of the pulverized coal particle in the hot gaseous medium is not possible. This minimum limiting particle diameter decreases with an increase in free stream gas phase temperature and in the volatile matter content of the coal particle.
- The thermodynamic irreversibilities in the process of combustion of a pulverized coal particle are due to chemical reaction and coupling effect of heat and mass transfer in gas phase. The irreversibility rate in the process is initially very low but it suddenly shoots up to a high value at the onset of ignition followed by a sharp rise and then gradual decrease to a final steady state value.

References

[1] R.C. Flagan, D.D. Taylor, Laboratory studies of submicron particles from coal combustion, in: 18th International Symposium on Combustion, The Combustion Institute, 1981, pp. 1227–1237.

[2] W.J. McLean, D.R. Hardesty, J.H. Pohl, Direct observations of devolatilizing pulverized coal particles in a combustion environment, in: 18th International Symposium on Combustion, The Combustion Institute, 1981, pp. 1239–1248.

[3] W.R. Seeker, G.S. Samuelsen, M.P. Heap, J.D. Trolinger, The thermal decomposition of pulverized coal particles, in: 18th International Symposium on Combustion, The Combustion Institute, 1981, pp. 1213–1226.

[4] M. Neville, R.J. Quann, B.S. Haynes, A.F. Sarofim, Vaporization and condensation of mineral matter during pulverized coal combustion, in: 18th International Symposium on Combustion, The Combustion Institute, 1981, pp. 1267–1274.

[5] D.P. Rees, L.D. Smoot, P.O. Hedman, Nitrogen oxide formation inside a laboratory pulverized coal combustor, in: 18th International Symposium on Combustion, The Combustion Institute, 1981, pp. 1305–1311.

[6] J.T. Kelly, B.A. Brown, J.B. Wightman, Pilot-scale development of a low-NO_x coal-fired tangential system, in: 18th International Symposium on Combustion, The Combustion Institute, 1981, pp. 1275–1283.

[7] K.W. Ragland, T.C. Jehn, J.T. Yang, Coal combustion at high Reynolds number, in: 18th International Symposium on Combustion, The Combustion Institute, 1981, pp. 1295–1303.

[8] T.W. Lester, W.R. Seeker, J.F. Merklin, The influence of oxygen and total pressure on the surface oxidation rate of bituminous coal, in: 18th International Symposium on Combustion, The Combustion Institute, 1981, pp. 1257–1265.

[9] D.R. Kassoy, P.A. Libby, Activation energy asymptotics applied to burning carbon particles, Combustion and Flame 48 (1982) 287–301.

[10] P.E. Unger, E.M. Suuberg, Modeling the devolatilization behavior of a softening bituminous coal, in: 18th International Symposium on Combustion, The Combustion Institute, 1981, pp. 1203–1211.

[11] P.J. Smith, T.H. Fletcher, L.D. Smoot, Model for pulverized coal-fired reactors, in: 18th International Symposium on Combustion, The Combustion Institute, 1981, pp. 1285–1293.

[12] A. Williams, M. Pourkashanian, J.M. Jones, L.A. Rowlands, A review of NO_x formation and reduction mechanisms in combustion systems, with particular reference to coal, J. Inst. Energy 70 (1997) 102–113.

[13] G. Löffler, D. Andahazy, C. Wartha, F. Winter, H. Hofbauer, NO_x and N_2O formation mechanisms—a detailed chemical kinetic modeling study on a single fuel particle in a laboratory-scale fluidized bed, J. Energy Resour. Tech., ASME 123 (3) (2001) 228–235.

[14] A. Arenillas, R.I. Backreedy, J.M. Jones, J.J. Pis, M. Pourkashanian, F. Rubiera, A. Williams, Modelling of NO formation in the combustion of coal blends, Fuel 81 (2002) 627–636.

[15] J.R. Fan, X.H. Liang, L.H. Chen, K.F. Cen, Modeling of NO_x emissions from a W-shaped boiler furnace under different operating conditions, Energy 23 (12) (1998) 1051–1055.

[16] R. Hurt, J.K. Sun, M. Lunden, A kinetic model of carbon burnout in pulverized coal combustion, Combustion and Flame 113 (1998) 181–197.

[17] B. Coda, L. Tognotti, The prediction of char combustion kinetics at high temperature, Exp. Therm. Fluid Sci. 21 (2000) 79–86.

[18] J. Görres, U. Schnell, K.R.G. Hein, Trajectories of burning coal particles in highly swirling reactive flows, Int. J. Heat Fluid Flow 16 (1995) 440–450.

[19] A. Williams, R. Backreedy, R. Habib, J.M. Jones, M. Pourkashanian, Modelling coal combustion: The current position, Fuel 81 (2002) 605–618.

[20] Z.Q. Li, F. Wei, Y. Jin, Numerical simulation of pulverized coal combustion and NO formation, Chem. Engrg. Sci. 58 (2003) 5161–5171.

[21] A. Williams, M. Pourkashanian, J.M. Jones, Combustion of pulverized coal and biomass, Prog. Energy Combust. Sci. 27 (2001) 587–610.

[22] L.D. Smoot, A decade of combustion research, Prog. Energy Combust. Sci. 23 (1997) 203–232.

[23] L.D. Smoot, Modeling of coal combustion processes, Prog. Energy Combust. Sci. 10 (1984) 229–272.

[24] H. Akoi, H. Nogami, H. Tsuge, T. Miura, T. Furukawa, Simulation of transport phenomena around the raceway zone in the blast furnace with and without pulverized coal injection, ISIJ Internat. 33 (6) (1993) 646–654.

[25] Y.C. Guo, C.K. Chan, K.S. Lau, Numerical studies of pulverized coal combustion in a tubular coal combustor with slanted oxygen jet, Fuel 82 (2003) 893–907.

[26] Y. Gordon, V. Shvidkiy, Y. Yaroshenko, N. Spirin, V. Lavrov, D. Shvidkiy, Blast Furnace models to analyze raceway zone formation and to predict lining life, in: ICSTI/Ironmaking Conference Proceedings, 1998, pp. 351–361.

[27] S.K. Som, S.S. Mondal, S.K. Dash, Energy and exergy balance in the process of pulverized coal combustion in a tubular combustor, ASME J. Heat Transfer 127 (Dec. 2005) 1322–1333.

[28] N. Lior, W.S. Darkin, H.S. Al-Sharqawi, The exergy fields in transport process: Their calculation and use, Energy 31 (2006) 553–578.

[29] S.K. Som, N.Y. Sharma, Energy and exergy balance in the process of spray combustion in a gas turbine combustor, ASME J. Heat Transfer 124 (2002) 828–836.

[30] N. Lior, Irreversibility in combustion, invited keynote paper Proc. ECOS '01: Efficiency, Costs, Optimization, Simulation and Environmental Aspects of Energy Systems, vol. 1, Istanbul, Turkey, 2001, pp. 39–48.

[31] A. Datta, S.K. Som, Thermodynamic irreversibilities and second law analysis in a spray combustion process, Combust. Sci. Technol. 142 (1999) 29–54.

[32] S.D. Hiwase, A. Datta, S.K. Som, Entropy balance and exergy analysis in the process of droplet combustion, J. Phys. D 31 (1998) 1601–1610.

[33] W.R. Dunbar, N. Lior, Sources of combustion irreversibility, Combust. Sci. Technol. 103 (1994) 41–61.

[34] S.K. Som, S.K. Dash, Thermodynamics of spray evaporation, J. Phys. D 26 (1993) 574–584.

[35] I.K. Puri, Second law analysis of convective droplet burning, Int. J. Heat Mass Transfer 35 (1992) 2571.

[36] S.K. Dash, S.P. Sengupta, S.K. Som, Transport processes and associated irreversibilities in droplet evaporation, J. Thermophys. Heat Transfer 5 (3) (1991) 366–373.

[37] S.K. Dash, S.K. Som, Transport processes and associated irreversibilities in droplet combustion in a convective medium, Int. J. Energy Res. 15 (1991) 603–619.

[38] M.N. Ozisik, Radiative Transfer and Interactions with Conduction and Convection, Wiley, New York, 1973.

[39] H. Kobayashi, J.B. Howard, A.F. Sarofim, Coal devolatilization at high temperatures, in: 16th International Symposium on Combustion, The Combustion Institute, 1976, pp. 411–425.
[40] M.M. Baum, P.J. Street, Predicting the combustion behavior of coal particles, Combust. Sci. Technol. 3 (1971) 231–243.
[41] M.A. Field, Rate of combustion of size-graded fractions of char from a low rank coal between 1200 K–2000 K, Combustion and Flame 13 (1969) 237–252.
[42] A. Bejan, Entropy Generation through Heat and Fluid Flow, Wiley–Interscience, New York, 1982.
[43] J.G. Krickwood, B. Crawford Jr., The macroscopic equation of transport, J. Phys. Chem. 56 (1952) 1048.
[44] J.O. Hirschfelder, C.F. Curtiss, R.B. Bird, Molecular Theory of Gases and Liquids, John Wiley, New York, 1954.
[45] R.C. Reid, J.M. Prausnitz, B.E. Poling, The Properties of Gases and Liquids, McGraw-Hill Book Company, New York, 1988.
[46] L.D. Smoot, D.T. Pratt, Pulverized Coal Combustion and Gasification, Plenum Press, New York, 1979.
[47] E.M. Sparrow, R.D. Cess, Radiation Heat Transfer, Hemisphere, Washington, DC, 1978.